SOIL LIQUEFACTION AND EFFECTS ON STRUCTURES; CASE STUDY IN ADIYAMAN-GÖLBAŞI AFTER THE 06 FEB 2023 EARTHQUAKES IN TÜRKİYE

Nurhan Ecemis*[1], Mustafa Karaman[2], Hadi Valizadeh[3], Cemalettin Dönmez[1], Korhan Deniz Dalgıç[1]

[1] İzmir Institute of Technology, Department of Civil Engineering, İzmir, Türkiye
[2] Karaman Engineering Project and Consultancy Co. İzmir, Türkiye
[3] Özyegin University, Department of Civil Engineering, İstanbul, Türkiye

nurhanecemis@iyte.edu.tr

Abstract. On 06 FEB 2023, two earthquakes occurred southeast of Türkiye; Kahramanmaraş-Pazarcık (M_w=7.8) and Kahramanmaraş-Elbistan (M_w=7.6). These earthquakes caused devastating effects in 11 cities in eastern Turkey and northern Syria. This study presents the post-earthquake discoveries in three liquefied areas during earthquakes and four buildings in these liquefied areas in the Gölbaşı District of Adıyaman City. First, an important role of post-earthquake piezocone penetration test (CPTu) in the characterization of subsurface conditions and assessment of liquefaction hazard is presented. Then, the effect of soil liquefaction on the performance of the buildings in these regions during the earthquake was investigated. These structures consist of 3- to 6-storys on raft foundations and exhibited various structural performances. Based on the interim findings from these areas, potential factors that cause moderate to severe damage to buildings were examined, and preliminary information on the relationship between soil properties, and the performance of buildings with shallow foundations in liquefied soil is presented.

Keywords: Soil Liquefaction, CPTu tests, Kahramanmaraş-Pazarcık and Elbistan earthquakes, Adiyaman-Gölbaşı, shallow foundations

1 Introduction

On 6th February 2023, at 04:17 a.m., local time, at the epicenter, a Kahramanmaraş-Pazarcık earthquake (M_w=7.8) followed by Kahramanmaraş-Elbistan earthquake (M_w=7.6) at 01:24 p.m. in Türkiye. The Kahramanmaraş-Pazarcık and Elbistan earthquakes' main shocks were at a focal depth of 8.6 km and 7 km, respectively [1]. After the main two shocks (Figure 1a), there were more than 400 aftershocks with magnitudes (M_w) greater than 4 (Figure 1b). Intensive damages were observed in buildings, transportation systems, earth structures, harbors, gas, water, and electricity lifelines. While a total of 11 nearby cities in Türkiye were heavily affected by the earthquakes, a localized-to-widespread, and minor-to-severe seismic liquefaction was observed in Hatay-İskenderun, Kahramanmaraş-Türkoğlu, and Adıyaman-Gölbaşı regions (highlighted areas in Figure 1c). These liquefaction case history sites provide insight into the post-Türkiye earthquake sequence liquefaction observations.

71% of the Gölbaşı District's critical infrastructure is damaged or completely devastated. Most buildings have suffered damage due to liquefaction as indicated by the yellow shaded zone in Figure 1d. In this area, a significant scale of the devastation became evident, with more than 1,350 buildings (1–8 stories) collapsed, and the rest of the buildings were significantly impacted by soil liquefaction. This paper explicitly presents the post-earthquake investigations at 3 liquefied sites and 4 buildings that were not damaged, moderately, and extensively damaged within the liquefied sites in Adiyaman-Gölbaşı during the 06 FEB 2023 earthquakes. The post-earthquake survey was performed on 17-22 JUNE 2023. First, the CPTu tests were conducted to determine the thickness and depth of the clay-like and sand-like layers. Soil strata that dominated the liquefaction-triggered conditions were examined from the soil behavior type index (I_c). By the soil type index, it is possible to predict if the soil behavior is controlled mainly by fines or sand since the cone responds to the in-situ mechanical behavior of the particular soil [2].

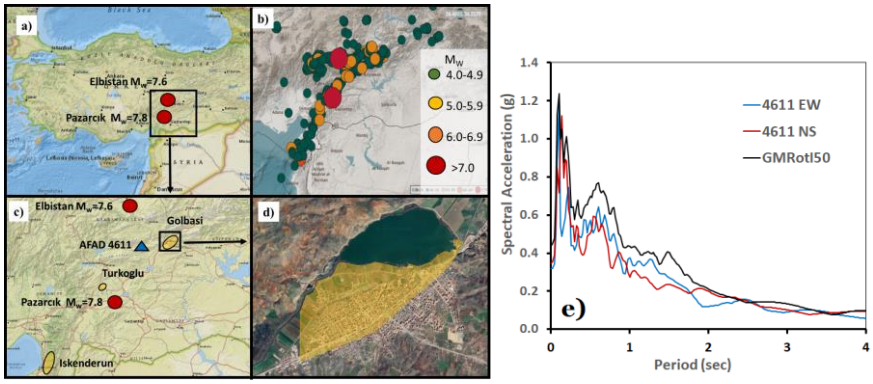

Fig 1. The 06 FEB 2023 earthquakes, M_w>7 (a) epicenters, (b) aftershocks with M_w>4, (c) the areas where the liquefaction occurred (highlighted in yellow), (d) the area where liquefaction was observed in the City of Golbasi (painted in yellow), and (e) spectral acceleration of station for E-W and N-S directions and calculated geometric mean

In inspected sites, a total of four 3 to 6-story buildings that are expected to respond in an approximately similar manner to earthquakes were emphasized to explain the damages detected due to seismic liquefaction and structural instability. The comparison between the measured differential settlements of structures and calculated post-liquefaction free-field settlements was investigated at each site. The basement floor elevations were measured from every corner of the buildings to find differential settlements of the structures. Also, the free-field level-ground settlement due to the liquefaction was estimated by using the post-liquefaction CPTu data proposed by [3]. Zhang et al. (2002) suggested a method between normalized tip resistance of CPT for clean sands $(q_{c1N})_{cs}$ and volumetric strain (ε_v) for varying safety factors against the liquefaction (FS_L= CRR/ CSR). Robertson and Wride (1998) recommended a method that CRR is the cyclic resistance ratio of clean sands directly related to $(q_{c1N})_{cs}$ and I_c, and CSR is the estimated cyclic stress ratio caused by an earthquake [4,5].

2 Earthquake shaking and seismic soil liquefaction investigation in Adıyaman-Gölbaşı

Kahramanmaraş-Pazarcık and Elbistan earthquakes' source-to-site distances (R) were 77 and 46 km, respectively. The earthquake records were gathered at the closest available station AFAD-4611 (Figure 1b), on a soil profile with shear wave velocity (V_s) of 730m/s. The distance between the station and Gölbaşı is nearly 46km. Instead of using both directions separately, the GMRotD50 method suggested by [6] was used to estimate the geometric mean ground motion of the Kahramanmaraş-Pazarcık earthquake. The spectral acceleration of the station for E-W and N-S directions and the calculated geometric mean of them are given in Figure 1e.

The soil around the lake contains 36% high plastic clay (CH), 24% low plastic clay (CL), 19% clayey sand (SC), 9% silty gravel (GM), and 7% silty sand (SM) [7]. The groundwater table (GWT) before the earthquakes was generally within 0.3 to 3.5m of the ground surface at the yellow area highlighted in Figure 1d. Outside of the zone of ground failure (in the southeast of the district, over the Gölbaşı-Adıyaman highway), clayey material with a very stiff structure and high plasticity is found below the GWT, which is about 7m.

The signs of seismic soil liquefaction in free-field, near the Gölbaşı lake zone, were observed in the form of sand/silt boiling (Figure 2a) and lateral spreading (Figure 2b). Earthquake-induced liquefaction can also severely damage infrastructures and buried pipelines in susceptible zones [8,9]. During the event, an embedded fuel tank of a gas station uplifted about 25cm due to liquefaction, as seen in Figure 2c. The street pavement cracking symptoms due to lateral spreading were also commonly observed.

Fig 2. Some of the seismic liquefaction symptoms (a) sand/silt volcanoes, (b) lateral spreading near the Golbasi Lake, and (c) fuel tank uplift in Gölbasi City Center

In addition to the free-field areas, great damage to buildings has been caused by liquefaction. The types of evidence due to liquefaction observed at the edges of residential buildings were sand volcanoes and lateral spreading. Many building foundations have also been subjected to excessive settlements (Figure 3a) and bearing capacity failures such as punching failure (Figure 3b) and overturning of the buildings due to seismic soil liquefaction. An extreme example of the overturning of a residential building in Gölbaşı-Adıyaman, as a result of exceeding the bearing capacity due to liquefaction, is shown in Figure 3c. The raft foundation thickness of this building was measured as 80cm. This building, which was lying on its side at the order of 15–20^{o} in the first earthquake, was subjected to rotation above the order of 35^{o} after the second earthquake and leaned on the structure behind it.

Fig 3. (a) Lateral spreading and excessive settlement, (b) punching failure, and (c) overturning of buildings in Gölbaşı

3 Field survey in Adıyaman-Gölbaşı

In this study, the field survey in three sites—Site A, Site B, and Site C—as satellite images are shown in Figure 4a. There were 3- to 6-story buildings on shallow foundations at these sites, including structures that performed satisfactorily to extensively damaged during the events. The response of buildings A-1 (at Site A), B-1, B-2 (at Site B), and C-1 (at Site C) to liquefied soil was investigated. The investigated structures (Table 1) were reinforced concrete (RC) structures on shallow/raft foundations without a basement and displayed interesting engineering performance characteristics.

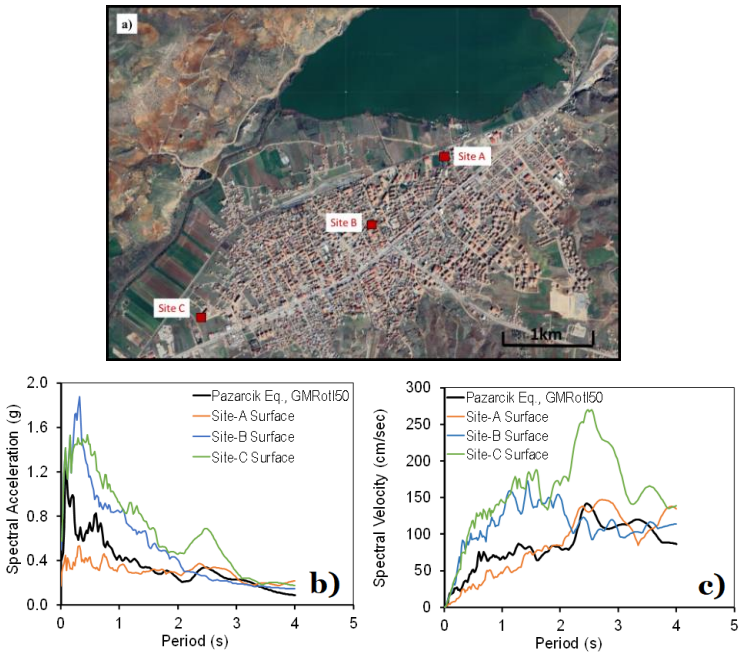

Fig 4. (a) Locations of 3 investigated sites, (b) acceleration, and (c) velocity response spectra at sites A, B, and C.

Within these three zones, the site soil was characterized after the earthquake with CPTu tests, which were performed near the buildings. The CPTu probe used had a 60° tip angle and 10 cm^2 tip area. The measured parameters were cone penetration resistance q_c, friction resistance f_s, and pore water pressures above the cone face (u_2 position) with a constant penetration speed of 2 cm/sec [10]. The soil behavior type index (I_c) was estimated by using the empirical relationship suggested by [11]:

$$I_c = \left[(3.47 - \log q_{c1})^2 + (\log F_r + 1.22)^2 \right]^{0.5} \quad (1)$$

$$F_r = \left[\frac{f_s}{q_c - \sigma_{vo}} \right] 100\% \quad (2)$$

$$q_{c1} = q_c \left[\frac{P_a}{\sigma_{vo}'} \right] \quad (3)$$

where P_a =1atm and σ_{vo} and σ_{vo}' is the total and effective vertical stress, respectively. I_c=2.6 is used to separate sandy and silty soils from clayey soils. Also, the free-field level-ground settlements due to the liquefaction were calculated using the post-liquefaction CPTu data suggested by [3].

To estimate the Peak Ground Acceleration (PGA) and Velocity (PGV) at the sites, GMRotI50 data shown in Figure 1c were firstly converted to usable data suggested by the Turkish Building Earthquake Code, TBEC [12] for V_s of 730m/s soil zone, then it was used for the 1D seismic response of the soil profile for each site. The elastic acceleration response spectra on the ground surface at each site are shown in Figures 4b and c. The maximum PGV value of Station 4611 is about 40 cm/sec. The PGV values are estimated to be 118, 120, and 108cm/sec for Sites A, B, and C, respectively. It indicates that even though the PGA values tend to drop for Site A, PGV values of all sites are comparable, and there is a heavy damage potential of the ground motions in all sites.

Table 1 Some information and measured properties of the three studied areas and structures

Site	A	B		C
Location coordinates	37.79198° N 37.64886° E	37.7872° N 37.6421° E		37.78037°N 37.6284° E
Building Name	A-1	B-1	B-2	C-1
Number of storey	4	3	6	6
Height of the building, H (m)	10.5	9.5	18.5	20.5
Construction year	2022	2022	2022	2022
Fundemental period of building in sec (TBEC 2018), ($T=0.07H^{0.75}$)	0.43	0.37	0.62	0.67
Soil improvement	Jet grout	No	No	Grouting
Lateral load resisting system (TBDY, 2018)	A33	A15	A15	A15
Geotechnical damage type	No tilt and settlement	Only local settlement	Tilt and settlement	Tilt and settlement
Calculated differential settlements at free-field (cm)	6.95	8.55	8.55	2.5
Structure tilt (Degree)	0	0.34° (E-W)	0.75° (N-S) 3.03° (E-W)	0.25° (N-S) 0.95° (E-W)
Measured differential settlements at structure (cm)	0	2(N-S) 10 (E-W)	16 (N-S) 100.5 (E-W)	8 (N-S) 23 (E-W)

3.1 Site A

The A-1 building (at Site A) is a 4-story, 10.5-m high structure, which is 16m wide (E-W) and 31.35m long (N-S) (Figure 5). It is known that it was started to construct in 2022. The foundation consists of a 0.6-m thick raft foundation and is embedded 1.4-m deep. The jet grout columns with a diameter of 100cm, length of 30m, and grid value of 1.50m were applied before construction. No significant building movement, structural or geotechnical damage is noted after the events.

The soil profile was examined in the upper 7.5m below-ground surface with the q_c, f_s, and Δu_2 profiles (Figures 6a–b–c). Site A's GWT was about 0.21m below the ground surface. Figure 6d shows the soil stratigraphy accomplished by the charts that linked cone parameters to soil type. Based on CPT-based soil type, the sand-like soils written in red (shown in Figure 6d), tend to have I_c<2.61, which is believed to be

liquefiable [5]. The shallow liquefiable clean sand to SM layer (I_c from 1.31 to 2.05) as well as the thin stratified SM to sandy silt layers (I_c from 2.05 to 2.6) are the critical layers that may liquefy [5].

Fig 5. Building A-1 right after the 06 FEB 2023 earthquakes (37.79198°N, 37.64886°E)

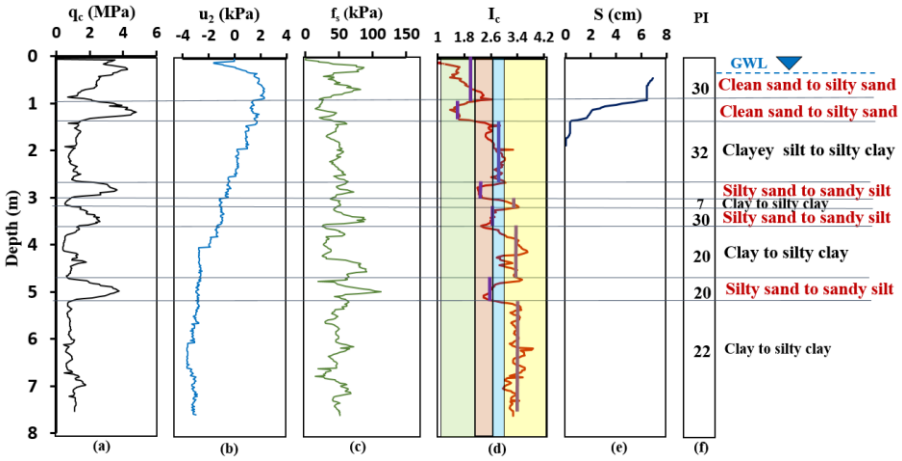

Fig 6. (a) Cone penetration resistance, (b) friction resistance, (c) pore water pressure versus depth, (d) soil behavior type index based on interpretation from CPTu, e) calculated free-field settlement according to [3], and f) PI and soil type according to [11] at Site A.

Moreover, the post-liquefaction volumetric reconsolidation settlement at the free field up to 2m depth was calculated [3] and plotted in Figure 6e. The settlement at the ground surface was calculated to be 69.5mm. No liquefaction manifestation was observed at Site A. According to the laboratory tests before the earthquake, from 1.5m to 2.5m, the average plasticity index (PI) was determined as 32. From 5.0 to 7.5m, the average PI is determined as 20 (Figure 6f). There was no settlement measured at building A-1 (Table 1). The improvement of the foundation soil below the building by jet grout columns can be the reason for having no manifestation of liquefaction failure at the building.

3.2 Site B

At site B, the geotechnical investigation and building construction design of two separate structures, B-1 and B-2, were investigated. The buildings were approximately 830m away from the lake. Before the events, the construction of the B-1 building had progressed up to the third-floor level, and the B-2 structure (freshly completed in 2023) consisted of a ground floor, five stories, and a roof. Notably, even though the structural frames are separated by an expansion joint, the B-1 and B-2 structures were established upon a unified 0.7m thick raft foundation (Figure 7a). The ground floor slab is 150mm thick. There were no applied soil improvements before the earthquakes below the buildings. After the earthquakes, severe liquefaction signs were observed throughout Site B, especially along the side of the B-2 building.

The soil profile was examined in the upper 5.2m below-ground surface with the q_c, f_s, and u_2 profiles (Figures 8a–b–c). The GWT depth at Site B was 0.15m. Based on the I_c–depth shown in Figure 8d, this site had a highly stratified profile. The sand-like soils written in red, tend to have I_c<2.61, which is believed to be liquefiable [5]. Moreover, the post-liquefaction volumetric reconsolidation settlement at the free field up to 3.3m depth was calculated [3] (Figure 8e). The settlement at the ground surface was calculated to be 85.5mm. The liquefaction manifestation as bulging and settlement of the soil was observed at Site B. The S-E and S-W corners of the B-2 structure settled 116cm and 15cm, respectively, relative to the structure's N-W corner. The structure settled differentially about 116cm toward the S-E edge. The building tilted 3.03^o to the east (Figure 7a) and 0.75^o to the south (Figure 7b). The PI was measured 35 at SM to the sandy silt layer. This shows that the soils with high PI>10% can also liquefy.

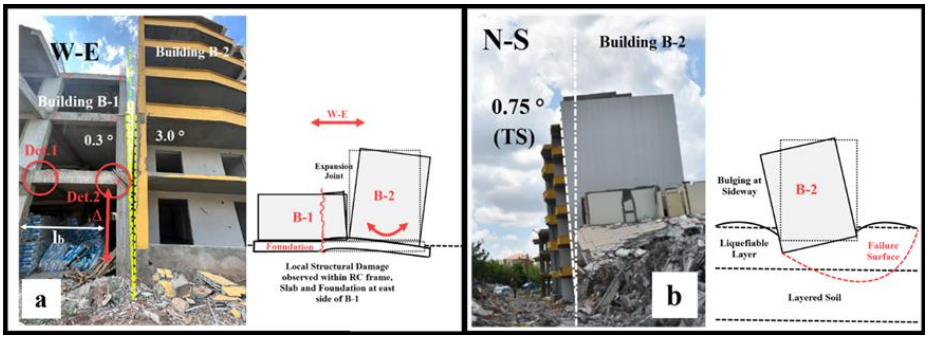

Fig 7. Photo and schematic view of liquefaction-induced displacement mechanism (a) B-1 and B-2 buildings, E-W direction, and (b) B-2 through N-S direction (37.7872°, 287 37.6421°)

Notwithstanding the substantial geotechnical damages, such as notable total and differential settlements and tilt in the B-2 building, structural damage was not readily visible within the context of the structure. However, structural damages in building B-1 at the neighboring span to building B-2 were observed. Noticeable indications of substantial geotechnical damage were not witnessed within the B-1 structure. The observed damage in the building supports that due to the dynamic motion and rota-

tional response of the B-2 building during the seismic event, considerable damage was created at the adjacent B-1 structure. The structural damage in the B-1 building indicates a major downward movement on the east side of the building (Figure 7a). The localization of the damage to a limited area and with the defined mechanism at the boundary with the B-2 building shows that this damage is not due to the ground motion demands. The remarkable rotation of B-2 and shear failure of soil caused a tilt of 0.34^{o} between B-1 and B-2 frames (Table 1).

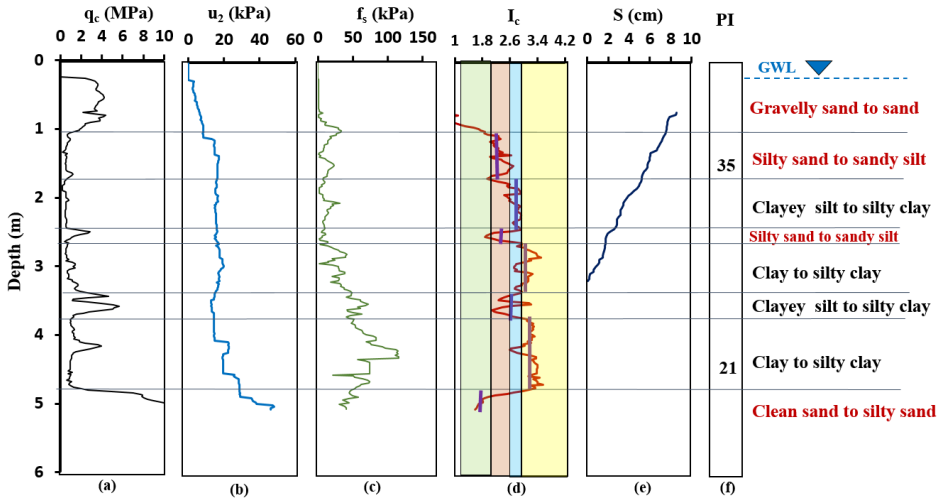

Fig 8. (a) Cone penetration resistance, (b) friction resistance, (c) pore water pressure versus depth, (d) soil behavior type index based on interpretation from CPTu, e) calculated free-field settlement according to [3], and f) PI and soil type according to [11] at Site B.

3.3 Site C

At Site C, the geotechnical investigation and building construction design of one 6-story residential building, C-1 (Figure 9a), which was freshly constructed and moderately damaged, was investigated. Building C-1 was approximately 1700m southwest of the lake, with a GWT depth of about 0.1m. The structure was supported on a raft foundation with a thickness of 160cm. In the vicinity of the site, there were two more similar six-story buildings. Grouting with a height of 6m and grid value of 2.5m was performed below the foundation.

The soil profile was examined by 6.2m deep CPTu test results (Figures 10a–b–c). Based on the I_c shown in Figure 10d, this site had the same soil profile from 2.5 to 6.2m. The sand-like soils which are believed to be liquefiable were written in red [5]. Moreover, the post-liquefaction volumetric reconsolidation settlement at the free-field up to 6m depth was calculated [3] (Figure 10e). The settlement at the ground surface was calculated to be 25mm. The liquefaction manifestation as bulging, settlement,

and sand boiling was observed at Site C. The PI was measured 9 at SM to sandy silt layer.

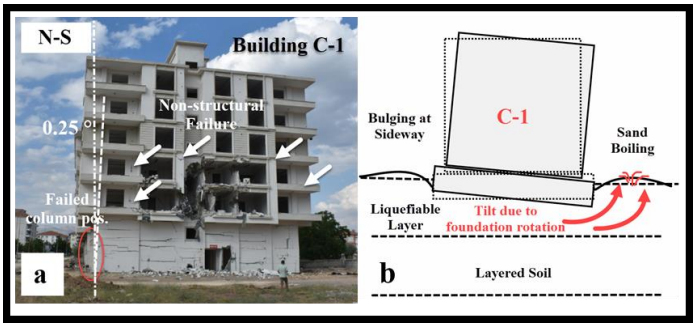

Fig 9. Building C-1 after the 06 FEB 2023 earthquakes, a) photo and b) schematic view of tilt in N-S direction due to geotechnical and structural damages (37.78037°, 37.6284°)

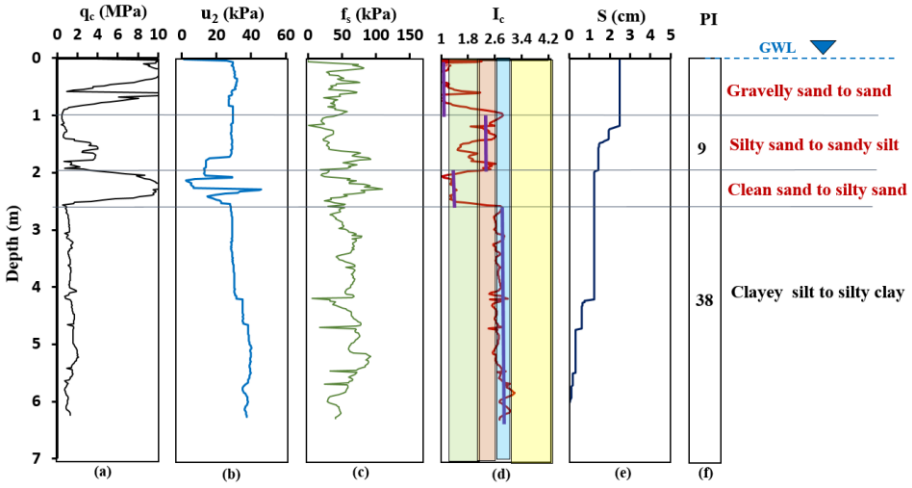

Fig 10. (a) Cone penetration resistance, (b) friction resistance, (c) pore water pressure versus depth, (d) soil behavior type index based on interpretation from CPTu, e) calculated free-field settlement according to [3], and f) PI and soil type according to [11] at Site C.

Following the events, severe liquefaction of the foundation soils induced significant total and differential settlements of the building, leading to structural distortions and cracking. The differential settlement of 8cm was observed at the S-E corner of the structure relative to its N-W corner. Furthermore, this building experienced displacement towards the north (23mm). The building tilt obtained from the differential settlement at the foundation corners was reported as 0.95° (toward west) and 0.25° (toward south) (Table 1). Severe levels of liquefaction-induced sand/silt ejecta were observed around the structure. Additionally, lateral spreading phenomena were detected on the vacant land on the southern side of the building.

4 Findings and Conclusions

Significant liquefaction-prone ground failures and building damages were observed in the Adıyaman-Gölbaşı District after the Kahramanmaraş-Pazarcık and Elbistan earthquakes. The findings and conclusions after the field survey are given below:

1. The post-liquefaction volumetric reconsolidation settlement at the ground surface at sites A, B, and C was calculated to be 69.5mm, 85.5mm, and 25mm, respectively [3]. This estimation shows that one can expect more liquefaction manifestation at Site A and B than Site C. However, liquefaction manifestations observed at sites B and C were not observed at Site A.
2. Based on the interim findings from the sites, the shallow liquefiable gravelly sand, and SM to sandy silt layers at the sites was the critical layer in the observed liquefaction. Moreover, Sites A and B are determined as highly stratified soils that are the critical layers that may liquefy [5]. The settlement observed at the free-field can be attributed to the coefficient of consolidation (c_v) and the thickness of the non-liquefiable soil layers, which are too thick to reduce the change in pore-water-pressure generation by time [14].
3. For a constant relative density, D_r, and FC, cone penetration resistance alone is insufficient to evaluate the liquefaction resistance due to the plasticity characteristics of fines [16] and the c_v of the soil [17]. FC affects the drainage, compressibility, and coefficient of consolidation of soil and, therefore, influences the u_2 and q_c that occur around the CPTu probe [17]. At each site, the PI values of the soils are very high. This case study shows that the soil layers with high PI can also liquefy [16].
4. The A-1 building, whose construction site had been improved using jet grout columns, showed almost no structural damage. Building B-1 is not damaged directly due to liquefaction and ground motion demands on its frame. However, the shared raft foundation with the neighboring B-2 building caused transmission of strong vertical movements and bending effects from one building to another, leading to localized extensive structural damage in one of its frames. C-1 that were supported on shallow foundations were affected by the liquefaction.

Funding

This study was supported by the Scientific and Technological Research Council of Turkey-TUBITAK [grant number 123M170].

References

1. AFAD (Disaster and Emergency Management Department), 2023 6th February 2023 Pazarcık-Elbistan Earthquakes in Kahramanmaraş (Mw:7-Mw:7.6) Report.

2. Robertson PK. CPT interpretation – a unified approach, Canadian Geotechnical Journal 2009, 46: 1-19.
3. Zhang G, Robertson PK, Brachman RWI. Estimating liquefaction-induced ground settlements from CPT for level ground. Can Geotech J 2002; 39: 1168–80.
4. Youd TL, Idriss IM. Proceeding of the NCEER Workshop on Evaluation of Liquefaction Resistance of Soils. Buffalo, NY: National Center for Earthquake Engineering Research, State University of New York at Buffalo, 1997.
5. Robertson PK, and Wride CE. Evaluating cyclic liquefaction potential using the CPT. Canadian Geotechnical Journal 1998, 35(3): 442-459.
6. Boore DM. Orientation-Independent, Nongeometric-Mean Measures of Seismic Intensity from Two Horizontal Components of Motion. Bulletin of the Seismological Society of America 2010, 100 (4): 1830–1835.
7. Akıl B, Akpınar K, Üçkardeşler C, Araz H, Sağlam M, Ecemis B, B. Uran Ş. Evaluation of Settlement Suitability of Gölbaşı (Adıyaman) Town, located on the East Anatolian Fault Zone Geological Bulletin of Turkey, 2008, 51(1).
8. Ecemis N, Valizadeh H, Karaman M. Sand-granulated-rubber mixture to prevent liquefaction induced uplift of buried pipes: A shaking-table study. Bull Earthq Eng 2021; 19: 2817–38.
9. Valizadeh H, Ecemis N. Soil liquefaction-induced uplift of buried pipes in sand-granulated-rubber mixture: Numerical modeling, Transportation Geotechnics 2022, Volume 33, 2022, 100719, ISSN 567 2214-3912.
10. ASTM D3441-16. Standard Test Method for Mechanical Cone Penetration Testing of Soils. 2018.
11. Robertson PK. Soil classification using the cone penetration test, Can. Geotech. J 1990. 27(1). 151-158.
12. Turkish Building Earthquake Code Posted: TBEC 2018 (TBDY, 2018. Türkiye Bina Deprem Yönetmeliği, Afet ve Acil Durum Yönetimi Başkanlığı, Ankara.)
13. Bird JF, Bommer JJ, Crowley H, Pinho R. Modelling liquefaction-induced building damage in earthquake loss estimation. Soil Dynamics and Earthquake Engineering 2006, 26: 15-30.
14. Ecemis N. Experimental and numerical modeling on the liquefaction potential and ground settlement of silt-interlayered stratified sands. Soil Dynamics and Earthquake Engineering 2021, Vol. (144), 106691, ISSN 0267-7261.
15. Ziotopoulou K, Cetin KO, Pelekis P Altun S, Klimis N, Sezer A, Rovithis E, Yılmaz M, Papadimitriou AG, Gulerce Z Can, G, Ilgac M, Cakır E, Soylemez B, Al-Suhaily A, Elsaid A, Zarzour M, Ecemis N, Unutmaz B, Kockar M, Akgun M, Kincal C, Bayat E, Ozener P, StewartJP, Mylonakis G. Geotechnical reconnaissance findings of the 30th October, 2020, Mw 7.0 Samos Island (Aegean Sea) earthquake" Bulletin of Earthquake Engineering 2022, 1573-1456.
16. Park SS, and KimYS. Liquefaction resistance of sands containing plastic fines with different plasticity, J. Geotech. Geoenviron. Eng. 2013, 139(5), 825-830.
17. Ecemis N, Karaman M. Influence of non/low plastic fines on cone penetration and liquefaction resistance, Engineering Geology 2014, Vol.181, 48-57.